 23 August, 2016

Recovery Model in Diode_CMC (Version 2.0.0 Level 2002)

Contents

History of the Documentation

02/Sep/2015 First release of Diode_CMC version 2.0.0 level 2002 documentation.

07/Oct/2015 Documentation corrected for Eqs. (20) and (21).

27/Oct/2015 Minor revision of documentation for ideal current and I_{total} in Appendix.

23/Aug/2016 Minor revision to include **FREV** and the in-code statement.

1. Introduction

The recovery model developed by Hiroshima University is based on the dynamic excess carrier distribution [1], where the dynamic carrier recombination process is modelled by applying the general NQS modelling technique developed by Hiroshima University [2]. The model is extended to high current-density conditions in [3]. Although the main target of the recovery model [1,3] is 1-dimentional vertical PiN diodes shown in Fig. 1a, the model is expected to be applicable to body diodes in lateral power MOSFETs as shown in Fig. 1b. Figure 2 shows all the equivalent circuits of the Diode_CMC model including the recovery model. Three RC networks (Figs. 2b, 2c and 2d) are included to model the dynamic carrier distribution. "A" and "K" in the figures represent the terminals "Anode" and "Cathode", respectively.

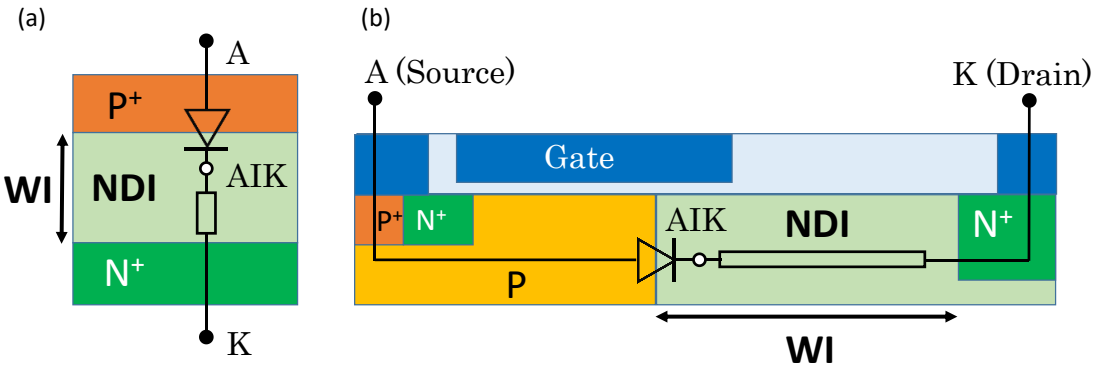

Fig. 1. Target device structures: (a) actual target, (b) example application.

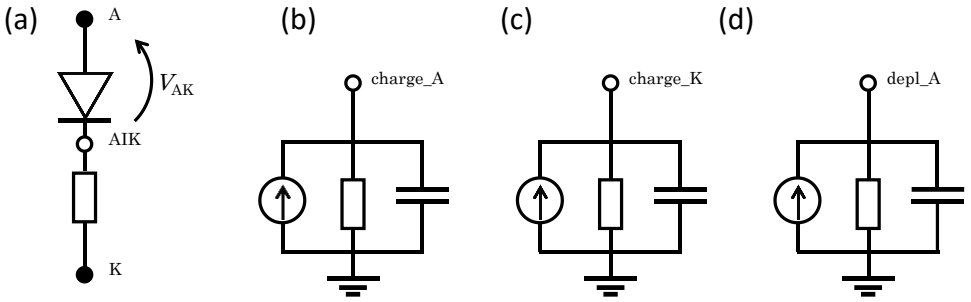

Fig. 2. Equivalent circuits. ("A" and "K" are the external terminal nodes.)

2. Summary of physics behind the recovery model

Figure 3a schematically shows the modelled static electron distribution profile along the drift region in the log scale under forward-biased DC condition. On the other hand, Fig. 3b shows the modelled static electron distribution in log scale under reverse-biased condition. Figure 4 schematically represents the modelled dynamic carrier distribution profile, where the NQS carrier dynamics is explicitly considered with $Q_{\mathrm{nexA,nqs}}$, $Q_{\mathrm{nexK,nqs}}$ and $W_{\mathrm{depA,nqs}}$. Physical quantities in the figures correspond to the model equations in Section 4 (e.g. "Q_nexA,nqs" corresponds to $Q_{\mathrm{nexA,nqs}}$ in Eq. (18)).

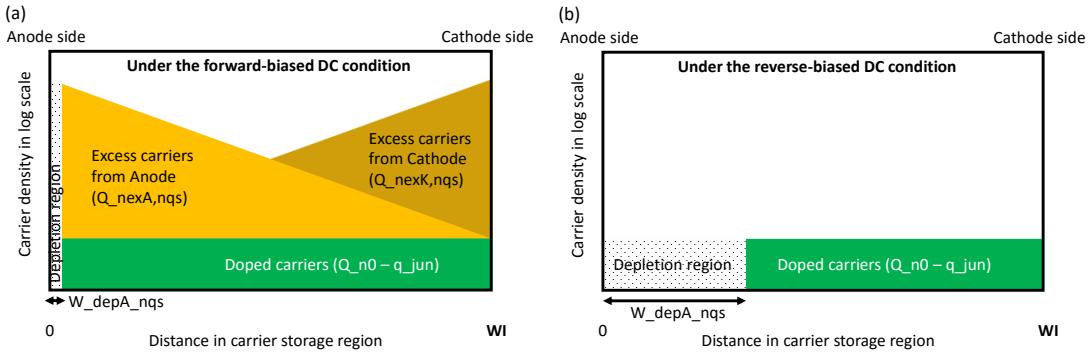

Fig. 3. Modelled carrier distributions under (a) forward and (b) reverse condition.

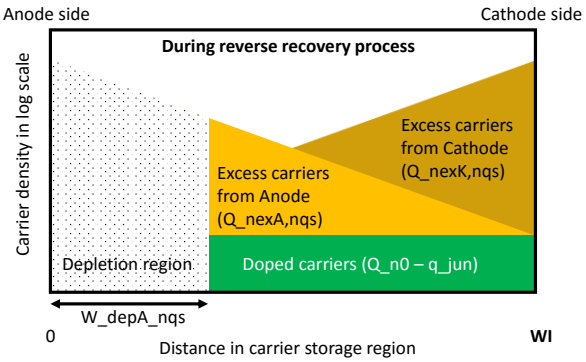

Fig. 4. Modelled carrier distribution during the reverse recovery process.

3. Model parameters and constants

Tables 1 to 4 summarize the parameters and constants referred to in this documentation.

Table 1. New parameters for recovery model (1 flag, 1 alias, 12 major & 1 minor (#)).

Name	Unit	Default	Min.	Max.	Description
CORECOVERY	-	0	0	1	Flag for recovery equations; 0=original model, 1=Hiroshima model
TNOM	C	21	-250	inf	Alias ref. temp. for **TRJ**
NJH	-	1.0	0.5	5.0	High-injection emission coefficient
NJDV	V^-1	0.1	0.0	1E6	Transition slope of emission coefficient
NDIBOT	cm^-3	1E16	1.0	1E23	Doping concentration of drift region (bottom)
NDISTI	cm^-3	1E16	1.0	1E23	Doping concentration of drift region (STI-edge)
NDIGAT	cm^-3	1E16	1.0	1E23	Doping concentration of drift region (gate-edge)
#**INJ1**	-	1.0	0.0	3.0	For recovery charge dens.
INJ2	-	10.0	0.0	20.0	For recovery charge dens. in high-injection condition
NQS	sec	5E-9	0.0	1E-3	Carrier delay time
TAU	sec	2E-7	0.0	1E-3	Carrier lifetime
WI	m	5E-6	0.0	1.0	Length of drift region
DEPNQS	sec	0.0	0.0	1E-3	Depletion delay time
TAUT	-	0.0	0.0	1.0E2	Temp. co. of carrier lifetime
INJT	-	0.0	0.0	20.0	Temp. co of high-inj density

* If **CORECOVERY**=0 (as default), the Diode_CMC original recovery model with **TT** works.

Table 2. Alias reference temperature **TNOM** for **TRJ**.

TRJ =	**TNOM Given**	**TNOM Not Given**
TRJ Given	TRJ	TRJ
TRJ Not Given	TNOM	TRJ Default

Table 3. Original Diode_CMC model parameters appearing in this documentation.

Name	Unit	Default	Min.	Max.	Description
NFABOT	-	1.0	0.1	Inf	ideality factor bottom comp
NFASTI	-	1.0	0.1	Inf	ideality factor STI-edge co.
NFAGAT	-	1.0	0.1	Inf	ideality factor gate-edge co.
TYPE	-	1	-1.0	1.0	Type param., in output val. 1 reflects n-type, -1 p-type
MULT	-	1	0	Inf	Num. of devices in parallel
AB	m^2	1E-12	0	Inf	Junction area
LS	m	1E-6	0	Inf	STI-edge pt. of junc. perim.
LG	m	0	0	Inf	Gate-edge pt. of junc. peri.
IDSATRBOT	Am^-2	1E-12	0.0	Inf	Sat. curr. dens. at the ref. temp. of bottom component
VBRBOT	V	10	0.1	Inf	Breakdown voltage of bottom component
VBRSTI	V	10	0.1	Inf	Breakdown voltage of STI-edge component
VBRGAT	V	10	0.1	Inf	Breakdown voltage of gate-edge component
RSBOT	VA^-1 m^2	0.0	0.0	Inf	Series resistance per unit-of-area of bottom comp.
RSSTI	VA^-1 m	0.0	0.0	Inf	Series resistance per unit-of-length of STI-edge comp.
RSGAT	VA^-1 m	0.0	0.0	Inf	Series res. per unit-of-length of gate-edge comp.
RSCOM	Ω	0.0	0.0	Inf	Common series resistance, no scaling

* **MULT**, **AB**, **LS** and **LG** are the instance parameters.

Table 4. Physical constants.

Symbol	Unit	Value	Description
n_{i0}	cm^-3	1.45E10	Intrinsic carrier density at 300K
μ_{p0}	cm^2/V/sec	500	Bulk hole mobility
μ_{n0}	cm^2/V/sec	1450	Bulk electron mobility
φ_{bi}	V	0.6	Built-in potential of P/N junction

* Other physical constants are defined in the original Diode_CMC model.

4. Model equations

4.1. DC current model with high injection

The high-injection model has been developed by Hiroshima University [3].

DC ideal current with high injection:

$$I'_D = (M_{\mathrm{ID}} - 1) \cdot I_{\mathrm{DSAT}} \tag{1}$$

$$M_{\mathrm{ID}} = \begin{cases} \exp\left[\dfrac{V_{\mathrm{AK}}}{n_{\mathrm{jA}}(V_{\mathrm{AK}}) \cdot \phi_{\mathrm{TD}}} + V_{\mathrm{HA}} \cdot \dfrac{n_{\mathrm{jA}}(V_{\mathrm{AK}}) - \mathbf{NFA}}{\mathbf{NFA} \cdot \mathbf{NJH}}\right] & if\ V_{\mathrm{AK}} < VMAX \quad (2a) \\ \left\{1 + \dfrac{V_{\mathrm{AK}} - VMAX}{\phi_{\mathrm{TD}}} \cdot dVMAX\right\} & \\ \cdot \exp\left[\dfrac{VMAX}{n_{\mathrm{jA}}(VMAX) \cdot \phi_{\mathrm{TD}}} + V_{\mathrm{HA}} \cdot \dfrac{n_{\mathrm{jA}}(VMAX) - \mathbf{NFA}}{\mathbf{NFA} \cdot \mathbf{NJH}}\right] & if\ V_{\mathrm{AK}} \geq VMAX \quad (2b) \end{cases}$$

$$dVMAX = \frac{n_{\mathrm{jA}}(VMAX) - VMAX \cdot \left[\dfrac{dn_{\mathrm{jA}}}{dV_{\mathrm{AK}}}\right]_{VMAX}}{n_{\mathrm{jA}}(VMAX)^2} + V_{\mathrm{HA}} \cdot \frac{\left[\dfrac{dn_{\mathrm{jA}}}{dV_{\mathrm{AK}}}\right]_{VMAX}}{\mathbf{NFA} \cdot \mathbf{NJH}} \tag{3}$$

where V_{AK} is the node voltage difference from AIK to A (see Fig. 2a). The ideal current I'_D corresponds to the same expression as in the JUNCAP2 documentation (see Eq. (4.36) of [4]). $I'_D, M_{\mathrm{ID}}, n_{\mathrm{jA}}, V_{\mathrm{HA}}, I_{\mathrm{DSAT}}$ and **NFA** are written in generic expressions which stand for the bottom, STI-edge and gate-edge components depending on the geometrical scaling (e.g. **NFA** stands for **NFABOT**, **NFASTI** and **NFAGAT**). For I_{DSAT} and $VMAX$, refer to the JUNCAP2 documentation (see Eqs. (4.16)-(4.18) and (4.22) of [4]). ϕ_{TD} is the thermal voltage at the device temperature.

Bias-dependent emission coefficients:

$$n_{\mathrm{jA,bot}} = \mathbf{NJDV} \cdot \left(V_{\mathrm{AK}} - V_{\mathrm{HA,bot}}\right) + \mathbf{NFABOT} \tag{4}$$

$$n_{\mathrm{jA,sti}} = \mathbf{NJDV} \cdot \left(V_{\mathrm{AK}} - V_{\mathrm{HA,sti}}\right) + \mathbf{NFASTI} \tag{5}$$

$$n_{\mathrm{jA,gat}} = \mathbf{NJDV} \cdot \left(V_{\mathrm{AK}} - V_{\mathrm{HA,gat}}\right) + \mathbf{NFAGAT} \tag{6}$$

where n_{jA} is limited within the range of **NFA** to **NJH** with smoothing functions.

High-injection threshold voltages on the Anode sides:

$$V_{\mathrm{HA,bot}} = \phi_{\mathrm{TD}} \cdot \mathbf{NFABOT} \cdot \ln\left(\frac{\mathbf{NDIBOT}}{p_{\mathrm{n0,bot}}}\right) \tag{7}$$

$$V_{\mathrm{HA,sti}} = \phi_{\mathrm{TD}} \cdot \mathbf{NFASTI} \cdot \ln\left(\frac{\mathbf{NDISTI}}{p_{\mathrm{n0,sti}}}\right) \tag{8}$$

$$V_{\mathrm{HA,gat}} = \phi_{\mathrm{TD}} \cdot \mathbf{NFAGAT} \cdot \mathbf{ln}\left(\frac{\mathbf{NDIGAT}}{p_{\mathrm{n0,gat}}}\right) \tag{9}$$

Minority carrier density at the thermal equilibrium:

$$p_{\mathrm{n0,bot}} = \frac{{n_{\mathrm{in}}}^2}{\mathbf{NDIBOT}} \tag{10}$$

$$p_{\mathrm{n0,sti}} = \frac{{n_{\mathrm{in}}}^2}{\mathbf{NDISTI}} \tag{11}$$

$$p_{\mathrm{n0,gat}} = \frac{{n_{\mathrm{in}}}^2}{\mathbf{NDIGAT}} \tag{12}$$

Intrinsic carrier density:

$$n_{\mathrm{in}} = n_{\mathrm{i0}} \cdot F_{\mathrm{TD,bot2}} \tag{13}$$

where $F_{\mathrm{TD,bot2}}$ is defined in the original part of Diode_CMC for cases when the ideal factor may take a value other than 1. Its simplified expression $F_{\mathrm{TD,bot}}$ is available for ideal current with ideality factor of 1 in JUNCAP2 documentation (see Eq. (4.13) of [4]).

4.2. Recovery model

Final diode branch current including the recovery effect:

$$I(A, AIK) = I_{\mathrm{j}} + \frac{dQ_{\mathrm{j}}}{dt} \tag{14}$$

where I_{j} is defined in the JUNCAP2 documentation (see Eq. (4.81) of [4]).

Total charge (depletion charge + recovery charge):

$$Q_{\mathrm{j}} = \mathbf{TYPE} \cdot \mathbf{MULT} \cdot \left(q_{\mathrm{jun}} + Q_{\mathrm{rr}}\right) \tag{15}$$

where the contribution of reverse recovery charge Q_{rr} is assigned to the total charge together with the junction charge, $q_{\mathrm{jun}} = \mathbf{AB} \cdot Q'_{\mathrm{j,bot}} + \mathbf{LS} \cdot Q'_{\mathrm{j,sti}} + \mathbf{LG} \cdot Q'_{\mathrm{j,gat}}$, modelled in the original Diode_CMC model (see Eq. (4.77) of the JUNCAP2 documentation [4]).

Total recovery charge (exported as an OP variable "qrr"):

$$Q_{\mathrm{rr}} = -\left(Q_{\mathrm{n0}} + Q_{\mathrm{nexA,nqs}} + Q_{\mathrm{nexK,nqs}}\right) \tag{16}$$

Electron charge at the thermal equilibrium:

$$Q_{\mathrm{n0}} = -\mathbf{AB} \cdot q \cdot \mathbf{NDIBOT} \cdot \mathbf{WI} \tag{17}$$

Excess charge injected from Anode:

$$\begin{aligned} Q_{\mathrm{nexA,nqs}} &= -\int_{W_{\mathrm{depA,nqs}}}^{\mathbf{WI}} q_{\mathrm{pexA,nqs}} \cdot \exp\left(-\frac{\mathrm{x}}{L_{\mathrm{a}}}\right) dx \\ &= -L_{\mathrm{a}} \cdot q_{\mathrm{pexA,nqs}} \cdot \left\{\exp\left(-\frac{W_{\mathrm{depA,nqs}}}{L_{\mathrm{a}}}\right) - \exp\left(-\frac{\mathbf{WI}}{L_{\mathrm{a}}}\right)\right\} \end{aligned} \tag{18}$$

Excess charge injected from Cathode:

$$\begin{aligned} Q_{\mathrm{nexK,nqs}} &= -\int_{W_{\mathrm{depA,nqs}}}^{\mathbf{WI}} q_{\mathrm{pexK,nqs}} \cdot \exp\left(-\frac{\mathbf{WI} - \mathrm{x}}{L_{\mathrm{a}}}\right) dx \\ &= -L_{\mathrm{a}} \cdot q_{\mathrm{pexK,nqs}} \cdot \left\{1 - \exp\left(-\frac{\mathbf{WI} - W_{\mathrm{depA,nqs}}}{L_{\mathrm{a}}}\right)\right\} \end{aligned} \tag{19}$$

Injected carrier densities:

$$\begin{aligned} q_{\mathrm{pexA}} = \mathbf{AB} \cdot q \cdot \Big\{ & p_{\mathrm{n0,bot}} \cdot exp_{\mathrm{A}} \cdot \mathbf{INJ1} \\ & \cdot \exp\left(-\mathbf{INJ2} \cdot (V_{\mathrm{AK}} - V_{\mathrm{HA}})^2 \cdot \exp\left(\mathbf{INJT} \cdot \ln\left(\frac{T_{\mathrm{KR}}}{T_{\mathrm{KD}}}\right)\right)\right) - p_{\mathrm{n0,bot}} \Big\} \end{aligned} \tag{20}$$

$$\begin{aligned} q_{\mathrm{pexK}} = \mathbf{AB} \cdot q \cdot \Big\{ & p_{\mathrm{n0,bot}} \cdot exp_{\mathrm{K}} \cdot \mathbf{INJ1} \\ & \cdot \exp\left(-\mathbf{INJ2} \cdot (V_{\mathrm{AK}} - V_{\mathrm{HK}})^2 \cdot \exp\left(\mathbf{INJT} \cdot \ln\left(\frac{T_{\mathrm{KR}}}{T_{\mathrm{KD}}}\right)\right)\right) - p_{\mathrm{n0,bot}} \Big\} \end{aligned} \tag{21}$$

where the NQS modelling technique is applied to q_{pexA} and q_{pexK}. Refer to Eqs. (32)–(39) for $q_{\mathrm{pexA,nqs}}$ and $q_{\mathrm{pexK,NQS}}$. T_{KR} and T_{KD} are reference temperature and device temperature, respectively.

Exponential quantities with the bias-dependent emission coefficients:

$$exp_{\mathrm{A}} = M_{\mathrm{ID,bot}} \tag{22}$$

$$exp_{\mathrm{K}} = \exp\left\{\beta \cdot \left[\frac{V_{\mathrm{AK}}}{n_{\mathrm{jK}}} - \frac{V_{\mathrm{HK}} - V_{\mathrm{HA}}}{n_{\mathrm{jK}}} + \frac{V_{\mathrm{HK}} \cdot (n_{\mathrm{jK}} - \mathbf{NFABOT})}{\mathbf{NFABOT} \cdot \mathbf{NJH}}\right]\right\} \tag{23}$$

where $M_{\mathrm{ID,bot}}$ is given in the DC current part with high injection.

Bias-dependent emission coefficient for the Cathode-side i/N junction:

$$n_{\mathrm{jK}} = \mathbf{NJDV} \cdot (V_{\mathrm{AK}} - V_{\mathrm{HK}}) + \mathbf{NFABOT} \tag{24}$$

where note that n_{jK} is limited within the range from **NFABOT** to **NJH** with smoothing functions.

High-injection threshold voltage on the Cathode side:

$$V_{\mathrm{HK}} = \phi_{\mathrm{TD}} \cdot \mathbf{NFABOT} \cdot \left\{ \ln\left(\frac{\mathbf{NDIBOT}}{p_{\mathrm{n0,bot}}} \right) + \frac{\mathbf{WI}}{L_{\mathrm{a}}} \right\} \tag{25}$$

Diffusion length:

$$L_{\mathrm{a}} = \sqrt{\tau_{\mathrm{HL}} \cdot D_{\mathrm{a}}} \tag{26}$$

$$\tau_{\mathrm{HL}} = \mathbf{TAU} \cdot \left(\frac{T_{\mathrm{KD}}}{T_{\mathrm{KR}}} \right)^{\mathbf{TAUT}} \tag{27}$$

Diffusion coefficients (including temp. dependence of phonon scattering):

$$D_{\mathrm{a}} = \frac{\mathbf{2} \cdot D_{\mathrm{n}} \cdot D_{\mathrm{p}}}{D_{\mathrm{n}} + D_{\mathrm{p}}} \tag{28}$$

$$D_{\mathrm{n}} = \phi_{\mathrm{TD}} \cdot \mu_{\mathrm{n0}} \cdot \left(\frac{T_{\mathrm{KD}}}{T_{\mathrm{KR}}} \right)^{-1.5} \tag{29}$$

$$D_{\mathrm{p}} = \phi_{\mathrm{TD}} \cdot \mu_{\mathrm{p0}} \cdot \left(\frac{T_{\mathrm{KD}}}{T_{\mathrm{KR}}} \right)^{-1.5} \tag{30}$$

Depletion width:

$$W_{\mathrm{depA}} = \sqrt{\frac{2\varepsilon_S}{q} \cdot \frac{\varphi_{\mathrm{bi}} - V_{AK}}{\mathbf{NDIBOT}}} \tag{31}$$

where the NQS modelling technique is applied to W_{depA} and gives $W_{\mathrm{depA,nqs}}$ later in the documentation. Refer to Eqs. (40)–(43).

4.3. NQS models for the recovery model

NQS model equation for the Anode-side excess carrier distribution:

$$q_{\mathrm{pexA,nqs}} = q_{\mathrm{pexA,nqs,prev}} + \frac{\Delta t}{\mathbf{NQS} + \Delta t} \cdot \left(q_{\mathrm{pex,A}} - q_{\mathrm{pexA,nqs,prev}} \right) \tag{32}$$

which is reduced to the differential equation form written as

$$\frac{q_{\mathrm{pex,A}}}{\mathbf{NQS}} = \frac{q_{\mathrm{pexA,nqs}}}{\mathbf{NQS}} + \frac{d\left(1 \cdot q_{\mathrm{pexA,nqs}}\right)}{dt} \tag{33}$$

The above equation is implemented in the RC network with “charge_A” (Fig. 2b) as

$$q_{\mathrm{pexA,nqs}} = V(\mathrm{charge\_A}) \tag{34}$$

$$I(charge\_A) = \frac{q_{\mathrm{pexA,nqs}} - q_{\mathrm{pex,A}}}{\mathbf{NQS}} + \frac{d\left(1 \cdot q_{\mathrm{pexA,nqs}}\right)}{dt} \tag{35}$$

NQS model equation for the Cathode-side excess carrier distribution:

$$q_{\mathrm{pexK,nqs}} = q_{\mathrm{pexK,nqs,prev}} + \frac{\Delta t}{\mathbf{NQS} + \Delta t} \cdot \left(q_{\mathrm{pex,K}} - q_{\mathrm{pexK,nqs,prev}}\right) \tag{36}$$

which is reduced to the differential equation form written as

$$\frac{q_{\mathrm{pex,K}}}{\mathbf{NQS}} = \frac{q_{\mathrm{pexK,nqs}}}{\mathbf{NQS}} + \frac{d\left(1 \cdot q_{\mathrm{pexK,nqs}}\right)}{dt} \tag{37}$$

The above equation is implemented in the RC network with "charge_K" (Fig. 2c) as

$$q_{\mathrm{pexK,nqs}} = V(\mathrm{charge\_K}) \tag{38}$$

$$I(charge\_K) = \frac{q_{\mathrm{pexK,nqs}} - q_{\mathrm{pex,K}}}{\mathbf{NQS}} + \frac{d\left(1 \cdot q_{\mathrm{pexK,nqs}}\right)}{dt} \tag{39}$$

NQS model equation for the depletion width:

$$W_{\mathrm{depA,nqs}} = W_{\mathrm{depA,nqs,prev}} + \frac{\Delta t}{\mathbf{DEPNQS} + \Delta t} \cdot \left(W_{\mathrm{depA}} - W_{\mathrm{depA,nqs,prev}}\right) \tag{40}$$

which is reduced to the differential equation form written as

$$\frac{W_{\mathrm{depA}}}{\mathbf{DEPNQS}} = \frac{W_{\mathrm{depA,nqs}}}{\mathbf{DEPNQS}} + \frac{d\left(1 \cdot W_{\mathrm{depA,nqs}}\right)}{dt} \tag{41}$$

The above equation is implemented in the RC network with "depl_A" (Fig. 2d) as

$$W_{\mathrm{depA,nqs}} = V(\mathrm{depl\_A}) \tag{42}$$

$$I(depl\_A) = \frac{W_{\mathrm{depA,nqs}} - W_{\mathrm{depA}}}{\mathbf{DEPNQS}} + \frac{d\left(1 \cdot W_{\mathrm{depA,nqs}}\right)}{dt} \tag{43}$$

5. Parameter extraction

Since the recovery model is based on the diode branch voltage V_{AK} (see Fig. 2a), modelling of the diode current and the series resistance is important before evaluating the recovery current. Figure 5 gives the reference result which is calculated with the default parameter set overwritten with **CORECOVERY**=1, **IDSATRBOT**=1E-6, **VBRBOT**=100, **VBRSTI**=100 and **VBRGAT**=100, where three measures are shown to evaluate the reverse recovery current. Two of the three measures ("(1) Recovery peak" and "(2) Magnitude of tail") shown in Fig. 5, are increased by increasing the initial recovery charge $Q_{\mathrm{rr,init}}$ stored in the drift region. $Q_{\mathrm{rr,init}}$ can be adjusted by the model parameters for the DC ideal current and some of the parameters for the recovery model (**TAU**, **WI**, **INJ2** and **INJ1**). Note that **TAU** cannot increase $Q_{\mathrm{rr,init}}$ in the case with the diffusion length longer than **WI**. Besides, $Q_{\mathrm{rr,init}}$ can be reduced by increasing the parameters for the saturation current (**IDSATRBOT**, etc.) because it lowers V_{AK} at the initial forward-biased state. The third measure ("(3) Recovery time") can be increased by the NQS carrier dynamics modelled with **NQS** and **DEPNQS**. Here the second measure is reduced at the same time. When the depletion width reaches **WI** after switching to the reverse-biased state, the recovery current suddenly turns down to zero. For temperature dependence, **TAUT** extends lifetime and then diffusion length, while **INJT** increases the carrier injection densities at the both junctions (P/i and i/N).

Table 5 shows a general parameter extraction scheme. For the physically-correct extraction, **INJ1** should be kept around 1.

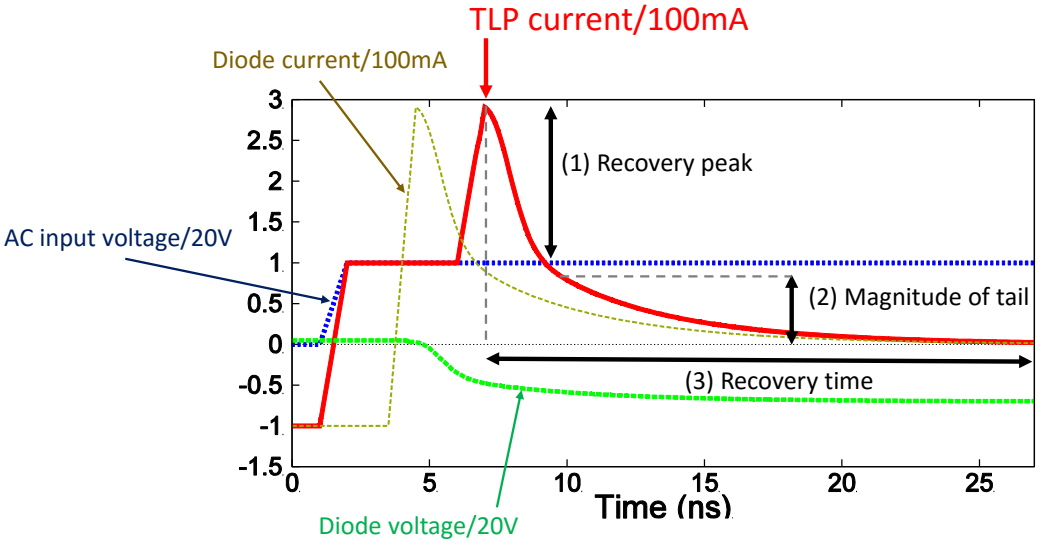

Fig. 5. TLP (transmission line pulsing) test result as a reference.

Table 5. General Extraction Scheme.

Step	Target Data	Parameters to be tuned
1	Reverse-biased AC C-V data (at different temperatures).	(Diode_CMC-original JUNCAP2 parameters)
2	DC I-V data at different temperatures.	Diode_CMC original parameters incl. **NFABOT**, **IDSATRBOT**, etc. for low-injection part; **NJH**, **NJDV**, **NDIBOT**, **NDISTI**, **NDIGAT** for high-injection part; **RSBOT**, **RSSTI**, **RSGAT**, **RSCOM** for resistive part
3	TLP data with small IF at low VR	**TAU**, **WI, NQS**, (**INJ1**=1.0)
4	TLP data with large IF at various VR	**INJ2**, **DEPNQS**
5	-	Repeat the steps 3 and 4
6	TLP data at different temperatures	**INJT**, **TAUT**

* IF and VR stand for the initial forward current and the final reverse voltage, respectively.

References

[1] J. Nakashima, M. Miyake, and M. Miura-Mattausch, "Dynamic-Carrier-Distribution-Based Compact Modeling of p-i-n Diode Reverse Recovery Effects," Jpn. J. Appl. Phys. (JJAP), vol. 51, 02BP06, pp. 1-4, Feb. 2012.

[2] D. Navarro, Y. Takeda, M. Miyake, N. Nakayama, K. Machida, T. Ezaki, H. J. Mattausch, M. Miura-Mattausch, "A Carrier-Transit-Delay-Based Nonquasi-Static MOSFET Model for Circuit Simulation and Its Application Harmonic Distortion Analysis," IEEE Trans. Electron Devices, Vol. 53, No. 9, pp. 2025-2034, Sept. 2006.

[3] M. Miyake, J. Nakashima, and M. Miura-Mattausch, "Compact Modeling of the p-i-n Diode Reverse Recovery Effect Valid for both Low and High Current-Density Conditions," IEICE Trans. Electron., Vol. E95-C, No. 10, pp. 1682-1688, Oct. 2012.

[4] A.J. Scholten, M. Durand, G.D.J. Smit, and D.B.M. Klaassen, *JUNCAP2: version 200.3*, Unclassified Report of NXP Semiconductors, NXP-R-TN-00000, April 2009.

Appendix A. Equation List from 1Q09 Subcommittee Report

These equations have been implemented into the Diode_CMC model in 2009, but were never documented.

- **Geometry scaling**

$$RS_{nom} = \frac{1}{\frac{AB}{RSBOT} + \frac{LG}{RSGAT} + \frac{LS}{RSSTI}} + RCOM$$

- **Temperature dependence of resistors**

$$RS = RS_{nom}\left(\frac{T}{TRJ}\right)^{STRS}$$

- **Thermal noise of resistors**

$$S_{id} = \frac{4kT}{RS}\Delta f$$

- **Temperature dependence of saturation current as a function of XTI (PT)**

$$I_{dsat}(T) = I_{dsat}(TRJ)\left(\frac{T}{TRJ}\right)^{XTI}$$

- **Ideal current**

$$I_{ideal} = I_{dsat}^{\frac{qV_{ak}}{NFACTOR*kT}}$$

- **Flicker noise**------*One common parameter (AF, KF) for all Area/STI/Gate components*

$$S_{id} = \frac{KF}{f} I_{total}^{AF}$$

- **Shot noise**

$$S_{id} = 2q[I_{ideal} + 2I_{dsat} + |I_{total} - I_{ideal}|]$$

where $I_{total} = I_{ideal} + I_{SRH} + I_{TAT} + I_{BBT}$. (see Eq. (4.72) of the JUNCAP2 doc. [4]).

- **Diffusion cap current**---*One common parameter for all Area/STI/Gate components*

$$I_{diffusion} = \frac{dI_{ideal}}{dt} TT$$

- **Breakdown voltage temperature equation**

$$VBR = VBR(TRJ) \times \left[1 + (T - TRJ) \times STVBR1 + (T - TRJ)^2 \times STVBR2\right]$$

Appendix B. Equation List of Additional Models

Following additional equation has been implemented into the Diode_CMC model since 2016.

- **Update of avalanche and breakdown (New model parameter: FREV)**

$$\alpha_{\mathrm{av}} = \frac{\mathbf{FREV} - 1}{\mathbf{FREV}}$$

where α_{av} is redefined with a new model parameter **FREV** (1E3 as default and backward compatible, ranging [1E3 : 1E10]). (see Subsection 3.2 and Eqs. (4.69) - (4.71) of the JUNCAP2 doc. [4])

Appendix C.

Silicon Integration Initiative (Si2)
Compact Model Coalition In-Code Statement

Software is distributed as is, completely without warranty or service support. NXP Semiconductors, Hiroshima University, and Silicon Integration Initiative, Inc. (Si2), along with their employees are not liable for the condition or performance of the software.

NXP Semiconductors, Hiroshima University, and Si2 own the copyright and grant users a perpetual, irrevocable, worldwide, non-exclusive, royalty-free license with respect to the software as set forth below.

NXP Semiconductors, Hiroshima University, and Si2 hereby disclaim all implied warranties.

NXP Semiconductors, Hiroshima University, and Si2 grant the users the right to modify, copy, and redistribute the software and documentation, both within the user's organization and externally, subject to the following restrictions

1. The users agree not to charge for the NXP Semiconductors, Hiroshima University, and Si2 -developed code itself but may charge for additions, extensions, or support.

2. In any product based on the software, the users agree to acknowledge NXP Semiconductors, Hiroshima University, and Si2 that developed the software. This acknowledgment shall appear in the product documentation.

3. Redistributions to others of source code and documentation must retain the copyright notice, disclaimer, and list of conditions.

4. Redistributions to others in binary form must reproduce the copyright notice, disclaimer, and list of conditions in the documentation and/or other materials provided with the distribution.

CMC In-Code Statement Revision 1.1 6/9/2016